REUCP, Petrópolis, Volume 14, n° 1 (2020), P. 12-24
ISSN 2318-0692

THERMAL ANALYSIS OF HEAT SINKS FOR ELECTRONIC COMPONENTS COOLING USING INTEGRAL TRANSFORMS

Lívia M. Corrêa* **and Daniel J. N. M. Chalhub**

Department of Mechanical Engineering, Group for Environmental Studies in Reservoirs - GESAR, Rio de Janeiro State University - UERJ, Rio de Janeiro, 20940-903, RJ, Brazil.

Keywords: Thermal Analysis, Heat sinks, Classical Integral Transform Technique, Electronic Components.

Abstract. This work proposes an approach using the Classical Integral Transform Technique (CITT) for the heat transfer analysis in heat sinks used in electronic components. One-dimensional fins and two-dimensional base formulations are solved separately, then, coupled to obtain the final solution of the system. Since the thickness of the base is small compared to other dimensions of the heat sink, a partial lumping approach in the z-direction is performed and the final mathematical formulation is two-dimensional. Additionally, at the bottom of the heat sink base, the heat flux coming from an electronic component is considered as the source term in the formulation. In order to obtain the final solution, the CITT is applied and four different cases are computed: the heat sink with zero, one, two and four fins. Finally, the results are obtained and analyzed. The convergence analysis showed that CITT has a great performance having no difficulties to obtain high accuracy with very few terms in the solution at positions away from the heat source, and required more terms near the chip. Moreover, the proposed approach has shown to be a good alternative method for this kind of problem.

E-mail addresses: livcorrea.uerj@gmail.com*, daniel.chalhub@eng.uerj.br.

1 INTRODUCTION

Heat transfer in Solid-State Electronics (SSE) is a rolling and critical issue in the design of modern electronic devices. Different industrial applications such as high-performance computers, aircraft, nuclear plant industries, and solar power applications use those chips for important functions and depend on the good performance of these components.

Over the years, SSEs have decreased in size and, with more internal components concentrated, have been requiring more power dissipation in order to ensure safe and efficient performance of the system. Peterson and Ortega [16] assert that the average component temperature must be maintained equal or below the manufacturer's maximum specified service temperature in order to guarantee an effective performance and long service life. In contrast, a violation of which can significantly compromise the reliability of the device. The failure rates of electronic components almost double when junction temperature increases by 10^oC beyond operating temperatures [12] and for these reasons, the cooling of electronic components have been substantially studied for over 30 years.

In 1988, Incropera [11] published a comprehensive review of convection cooling options in which different types of heat sinks are mentioned. The parallel plate heat sink can suffer some improvements for an enhanced heat transfer, which was largely described in the article. More recently, another review was performed by Adham et al. [1] devoted to enhancing the overall thermal and hydrodynamic performance of microchannel heat sinks. From this review, it can be drawn the growing interest in microchannel heat sinks asserting the development of research in this area.

The thermal dissipation promoted by heat sinks has motivated several works about analysis and optimization of fins in heat sinks. The work of Teertstra et al. [20] presented an analytical model to obtain the average heat transfer rate for forced convection, air cooled, plate fin heat sinks. The work of Lehtinen [13] analyzed both heat conduction and convection in fins applying well-known analytical and experimental results for convective heat transfer. The geometry of the fin was also studied for maximizing the heat transfer. The work of Ong et al. [15] analyzed different geometries of rectangular and cylindrical fins optimizations for maximum heat dissipation on electronic components. The behavior of different geometric parameter heat sinks with rectangular fins was also analyzed by Anselmo [2]. The work of Azarkish et al. [3] investigated the geometry of the longitudinal fins with variable cross-sectional area achieving its optimum fin profile using a genetic algorithm. On the other hand, Cuce and Cuce [9] tested different rectangular fins configurations to produce the maximum heat loss in a specific volume and length of fin numerically exposed to convection and radiation heat transfer.

Several recent works about heat sinks can be found in the literature, especially using analytical and numerical methodologies to evaluate the heat transfer promoted by the system. One can mention the research developed by Türkakar and Okutucu-Özyurt [21] in which a dimensional optimization of silicon heat sinks for located multiple heat sources by minimizing the thermal resistance at constant pumping power. In addition, the work of Singh et al. [18] used the LaPlace transform technique to solve the temperature distribution of 1D fin with internal heat generation and periodic boundary condition. The work [23] presents a heat transfer numerical simulation of a heat sink installed on a square chip of a computer using the fourth-order Runge-Kutta method to solve the non-linear heat transfer equation. Finally, the research developed by Malek and Shabani [14] simulates macro and microscope heat transfer utilizing different formulations for different scales. The used methodology is based on spectral methods, solving it numerically by spectral discretization and finite differences method. The microscope analysis uses the dual-

phase lag formulation and for the macroscope problems, based on the Fourier Law, commercial software was used for the simulations.

The Integral Transform Technique is a powerful method to solve differential equations and is classified as Classical (CITT) or Generalized (GITT). The CITT is an all analytical method and is mostly applied in linear problems [7]. The CITT method consists in the development of the appropriate transformation pair for the solution, then apply the integral transformation to remove the spatial partial derivatives, reducing it to an Ordinary Differential Equation, and solve the ODE under the boundary conditions. The temperature transformation is done by the inversion formula, where the desired solution is obtained. The GITT is a hybrid analytical-numerical technique and transforms nonlinear partial differential equation models to a coupled nonlinear system of ordinary differential equations (ODEs) to be solved numerically. Chalhub [6] enumerates some advantages of the Integral Transform Technique when compared to numerical methods such as the reduction in processing time, not having a mesh for discretization (the solution comes in a continuous domain) and faster convergence. Sphaier and Cotta [19] applied the Integral Transform Technique on the solution of a multidimensional partial differential model within irregularly shaped domains. Braga Junior and Sphaier [4] also applied the GITT in order to obtain the heat transfer solution in heterogeneous mediums such as Functionally Graded Materials with variable properties. The Integral Transform Technique has been previously applied to electronic problems. Dantas [10] have applied the GITT for the solution of heat transfer in microchips. An encapsulated microchip was considered with different thermal conductivity layers over the chip thickness. Recently, Corrêa and Chalhub [8] presented the solution of Solid-State Electronics with one heat generation on its domain and solved by Classical Integral Transform Technique. Furthermore, Pinheiro et al. [17] applied integral transforms for solving the conjugated radiation-conduction in a finned-tube configuration transient problem heat sinks.

This work proposes an analytical heat transfer approach to analyze heat sinks (HS) applied to dissipate the heat generated in electronic components. Fins and base formulations are solved separately, then, coupled to obtain the final solution of the system. First, the fin formulation is developed and solved, then, the effective heat transfer coefficient for the fin is obtained. This coefficient depends on the position of the fins and is used to obtain the solution for the base of the heat sink. On the bottom of the base of the heat sink, the heated solid-state electronic releases its heat on the HS to be dissipated. On the top of the base of the HS, the fins increase the heat dissipation to the environment and, consequently, enhance the cooling of the chip. Since the thickness of the base is small compared to other dimensions of the heat sink, a partial lumping approach in the z-direction is performed and the final mathematical formulation is two-dimensional, considering the heat flux arriving from the chip as a source term. In order to obtain the final solution of the base, the Classical Integral Transform Technique (CITT) is applied. In this case, however, the transformed equation cannot be solved analytically and requires a numerical discretization. A truncation error is involved since the infinite summation must be truncated. This error decreases as the number of summation terms (truncation order) are increased, and the solution converges to a final value. Four different layouts are considered: the heat sink with zero, one, two and four fins.

2 MATHEMATICAL FORMULATION FOR RECTANGULAR FINS

The formulation for the one-dimensional rectangular fins is obtained using the energy equation in steady-state [5]. The boundary conditions applied on the fin are fixed temperature at the

base of the heat sink (isothermal base) and convection at the fin longitudinal end:

$$\frac{\mathrm{d}^2T}{\mathrm{d}x_a^2} - \frac{P_a h}{k_a A_a}(T - T_f) = 0 \quad \text{for} \quad 0 \leq x_a \leq L_a, \tag{1a}$$

$$T|_{x_a=0} = T_b, \qquad -k_a \frac{\mathrm{d}T}{\mathrm{d}x_a}\bigg|_{x_a=L_a} = h(T(L_a) - T_f), \tag{1b}$$

where T is the temperature, x_a is variable for the fin, k_a is the thermal conductivity of the fin, A_a is the transversal area of the fin, P_a is the perimeter of the fin, h is the heat transfer coefficient by convection , L_a is the length of the fin, T_B indicates the temperature for the base and T_f is the temperature of the surrounding air. The subscript a is used to indicate variables and parameters related to the fin. Considering the thermal conductivity, the transversal area and perimeter constants: Considering the thermal conductivity, the transversal area and perimeter constants:

The nondimensionalization leads to the following mathematical formulation for the fin:

$$\frac{\mathrm{d}^2\Theta}{\mathrm{d}\xi_a^2} - m^2\Theta = 0 \quad \text{for} \quad 0 \leq \xi_a \leq 1, \tag{2a}$$

$$\Theta(0) = 1 \qquad \frac{\mathrm{d}\Theta}{\mathrm{d}\xi_a}\bigg|_{\xi_a=1} = -\mathrm{Bi}_a\Theta(1). \tag{2b}$$

The non-dimensional groups are defined as:

$$\xi_a = \frac{x_a}{L_a}, \quad \Theta = \frac{T - T_f}{T_b - T_f}, \quad \mathrm{Bi}_a = \frac{hL_a}{k_a}, \quad m^2 = \frac{Bi_a P_a L_a}{A_a}. \tag{3}$$

The solution for (2a) is:

$$\Theta(\xi_a) = \frac{m\cosh(m(1-\xi_a)) + Bi_a \sinh(m(1-\xi_a))}{m\cosh(m) + Bi_a \sinh(m)}. \tag{4}$$

The heat flux in each fin of the heat sink is:

$$\dot{q_a''} = -k_a(T - T_f)\frac{\mathrm{d}\Theta}{\mathrm{d}\xi_a}\bigg|_{\xi_a=0}, \tag{5}$$

leading to:

$$\dot{q_a}'' = k_a(T - T_f)\frac{m\,(\mathrm{Bi}_a\cosh(m) + m\sinh(m))}{m\cosh(m) + \mathrm{Bi}_a\sinh(m)} = h_{fin}(T - T_f). \tag{6}$$

Finally, the fin heat transfer coefficient h_{fin} is given by:

$$h_{fin} = k_a\frac{m\,(\mathrm{Bi}_a\cosh(m) + m\sinh(m))}{m\cosh(m) + \mathrm{Bi}_a\sinh(m)}. \tag{7}$$

3 PROBLEM FORMULATION

The mathematical formulation of the heat conduction at the base of the heat sink is given by the energy equation in steady-state after applying a partial lumping approach in z-direction.

For this work, a heat flux from the chip ($\dot{q_o}''$) acting over the heat sink is considered. The convection flux ($\dot{q_c}''$) occurs on the top surface of the heat sink without fins (Figure 1). On the other hand, where the fin is located, the heat flux is the fin heat flux from the fin ($\dot{q_a}''$) of the heat sink:

$$\dot{q}_h'' = \begin{cases} \dot{q_a}'' = h_{fin}(T - T_f) & \text{if } x_{ai_K} \leq x \leq x_{af_K} \\ \dot{q_c}'' = h_{conv}(T - T_f) & \text{if } x < x_{ai_K} \text{ or } x > x_{af_K} \end{cases}, \tag{8}$$

where the subscript i indicates where the fin length begins and f where it ends. The index k indicates which fin is evaluated and the subscript a is used to indicate positions related to the fin.

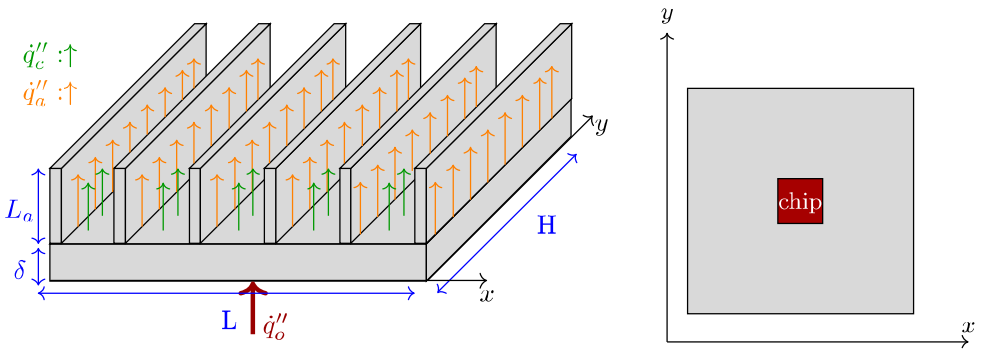

Figure 1: Schematic heat sink view and bottom of the base of the heat sink indicating the location of the chip

The definition of the effective heat transfer coefficient (h), as can be concluded, depends of its location on the base of the heat sink. On the region where the fins are located, h assume h_{fin} value and where there is only convection, h assume h_{conv} value:

$$h(x) = \begin{cases} h_{fin} & \text{if } x_{ai_K} \leq x \leq x_{af_K} \\ h_{conv} & \text{if } x < x_{ai_K} \text{ or } x > x_{af_K} \end{cases}. \tag{9}$$

The formulation is showed bellow with its respective boundary conditions:

$$k\left(\frac{\partial^2 T(x,y)}{\partial x^2} + \frac{\partial^2 T(x,y)}{\partial y^2}\right) = \frac{\dot{q}_h''(x)}{\delta} - \frac{\dot{q}_o''(x,y)}{\delta} \quad \text{for } 0 \leq x \leq L \text{ and } 0 \leq y \leq H, \tag{10}$$

$$\left.\frac{\partial T}{\partial x}\right|_{x=0} = 0, \quad \left.\frac{\partial T}{\partial x}\right|_{x=L} = 0, \quad \left.\frac{\partial T}{\partial y}\right|_{y=0} = 0, \quad \left.\frac{\partial T}{\partial y}\right|_{y=H} = 0, \tag{11}$$

where T is the temperature, k is the thermal conductivity of the base, $\dot{q}_o''$ is the heat flux from the chip to the heat sink, T_f is the environment air temperature, h is the convection heat transfer coefficient, x and y are the cartesian coordinates and L, H and δ are the dimensions of the heat sink in x, y and z directions respectively.

The nondimensionalization of the problem leads to the following mathematical formulation:

$$\frac{\partial^2 \Theta}{\partial \xi^2} + \frac{\beta^2 \partial^2 \Theta}{\partial \eta^2} - \text{Bi}(\xi)\gamma\Theta = -Q(\xi,\eta) \quad \text{for} \quad 0 \leq \xi \leq 1 \quad \text{and} \quad 0 \leq \eta \leq 1, \tag{12}$$

$$\left.\frac{\partial \Theta}{\partial \xi}\right|_{\xi=0} = 0, \quad \left.\frac{\partial \Theta}{\partial \eta}\right|_{\eta=0} = 0, \quad \left.\frac{\partial \Theta}{\partial \xi}\right|_{\xi=1} = 0, \quad \left.\frac{\partial \Theta}{\partial \eta}\right|_{\eta=1} = 0. \tag{13}$$

The non-dimensional groups are defined as:

$$\xi = \frac{x}{L}, \quad \eta = \frac{y}{H}, \quad \Theta = \frac{T - T_f}{T_b - T_f}, \tag{14}$$

$$\beta = \frac{L}{H}, \quad \gamma = \frac{L}{\delta}, \tag{15}$$

$$\mathrm{Bi}(\xi) = \frac{h(\xi)L}{k}, \quad Q(\xi, \eta) = \frac{\dot{q}_o'' L^2}{k\delta\Delta T}, \tag{16}$$

where β and γ are aspect ratios, $\mathrm{Bi}(\xi)$ is the Biot number and depends of ξ, Θ is the dimensionless temperature, ξ and η are the dimensionless versions of x and y, and Q is the heat flux acting over the domain from the chip to the base of the heat sink. The chip is located at the center of the base.

4 SOLUTION BY CLASSICAL INTEGRAL TRANSFORM TECHNIQUE

In order to solve the proposed problem, the Classical Integral Transform Technique (CITT) is applied. This is an analytical technique that uses expansions of the sought solution in terms of an infinite orthogonal basis of eigenfunctions, keeping the solution process always within a continuous domain. In order to establish the transformation pair, the temperature field is written as function of an orthogonal eigenfunctions obtained from the following auxiliary eigenvalue problem known as the Helmholtz classic problem in cartesian coordinates, where $\Psi(\eta)$ are the eigenfunctions and λ_n are the eigenvalues. For this particular problem, the case where λ= 0 also exists.

The solution of the equation (12) is defined as:

$$\Theta = \sum_{n=0}^{\infty} \frac{\bar{\Theta}_n(\xi)\Psi_n(\eta)}{N_n}, \tag{17}$$

where $\bar{\Theta}_n(\xi)$ and $\Psi_n(\eta)$ are the functions to be solved separally in order to find the temperature field and are eigenfunctions. $\bar{\Theta}_n(\xi)$ is also the transformed version of Θ. N_n is the norm and is defined as:

$$N_n = \int_0^1 \Psi_n^2 \mathrm{d}\eta. \tag{18}$$

In order to establish the transformation pair, the temperature field is written as functions of an orthogonal eigenfunctions obtained from the following auxiliary eigenvalue problem known as the Helmholtz classic problem in cartesian coordinates, where $\Psi(\eta)$ are the eigenfunctions and λ_n are the eigenvalues. For this particular problem, the case where $\lambda = 0$ also exists:

$$\Psi_n''(\eta) + \lambda_n^2 \Psi_n(\eta) = 0, \tag{19a}$$

$$\Psi_n'(0) = 0, \quad \Psi_n'(1) = 0. \tag{19b}$$

Solving the differential equation, the solution shows that the eigenfunction is formed by sines and cosines. Applying the boundary conditions, the term formed by sines is eliminated from the solution and the values of the eigenvalues λ_n are found.

For $\lambda = 0$, the solution of the eigenvalue problem is given by:

$$\Psi_0(\eta) = 1, \qquad \lambda_0 = 0, \tag{20}$$

and for $\lambda > 0$:

$$\Psi_n(\eta) = \cos(\lambda_n \eta), \qquad \lambda_n = n\pi \quad \text{for} \quad n = 1, 2, 3, \ldots \tag{21}$$

To apply the CITT, the transformation pair is defined:

$$\text{Transformation} \quad \Rightarrow \quad \bar{\Theta}_n(\xi) = \int_0^1 \Theta \Psi_n(\eta) \mathrm{d}\eta, \tag{22}$$

$$\text{Inversion} \quad \Rightarrow \quad \Theta = \sum_{n=0}^{\infty} \frac{\bar{\Theta}_n(\xi)\Psi_n(\eta)}{N_n}. \tag{23}$$

The equation (12) is written again, multiplied by Ψ_n and integrated in the domain for η. The objective in this step is obtain the transformed equation:

$$\int_0^1 \frac{\partial^2 \Theta}{\partial \xi^2} \Psi_n d\eta + \beta^2 \int_0^1 \frac{\partial^2 \Theta}{\partial \eta^2} \Psi_n d\eta - \mathrm{Bi}(\xi)\gamma \int_0^1 \Theta \Psi_n d\eta = -\int_0^1 Q \Psi_n d\eta. \tag{24a}$$

Finally, the transformed equation is obtained, after simplifications, for $\lambda > 0$:

$$\bar{\Theta}_n'' - (\beta^2 \lambda_n^2 + \mathrm{Bi}(\xi)\gamma)\bar{\Theta}_n = -\bar{Q}_n(\xi), \tag{25}$$

where $\bar{Q}_n$ is given by:

$$\bar{Q}_n(\xi) = \int_0^1 Q(\xi, \eta)\Psi_n(\eta)\mathrm{d}\eta. \tag{26}$$

The transformed boundary conditions are:

$$\bar{\Theta}_n'(0) = 0, \quad \bar{\Theta}_n'(1) = 0. \tag{27}$$

This equation cannot be solved analytically because of the dependence of ξ on Biot number. For this reason, the equation (25) is solved numerically using the NDSolve subroutine available on the software Mathematica 11.3 [22].

The transformed equation for $\lambda = 0$ is given by:

$$\bar{\Theta}_0'' - (\mathrm{Bi}(\xi)\gamma)\bar{\Theta}_0 = -\bar{Q}_0(\xi), \tag{28}$$

where $\bar{Q}_0$ is given by:

$$\bar{Q}_0(\xi) = \int_0^1 Q(\xi, \eta)\Psi_0(\eta)\mathrm{d}\eta = \int_0^1 Q(\xi, \eta)\mathrm{d}\eta. \tag{29}$$

The transformed boundary conditions are:

$$\bar{\Theta}_0'(0) = 0, \quad \bar{\Theta}_0'(1) = 0. \tag{30}$$

Once again, the equation cannot be solved analytically for the same previous reason and the equation (28) is solved numerically using the NDSolve subroutine.

Finally, in order to obtain the final temperature field, the inversion formula (23) must be utilized and the summation must be truncated to a finite value ($n_{\max}$).

5 RESULTS AND DISCUSSION

After describing the problem, the parallel plate fins formulation and the solution methodology, in this section the results are shown. For the chosen layouts, the heat sink (HS) presents a squared shape, therefore the ratio aspect $\beta = 1$. The value of the non-dimensional group $\mathrm{Bi}\gamma$ for convection is 0.1, and 3 for the regions where the fins are located. The dimensionless heat flux $Q(\xi, \eta)$ is plotted in figure 2a.

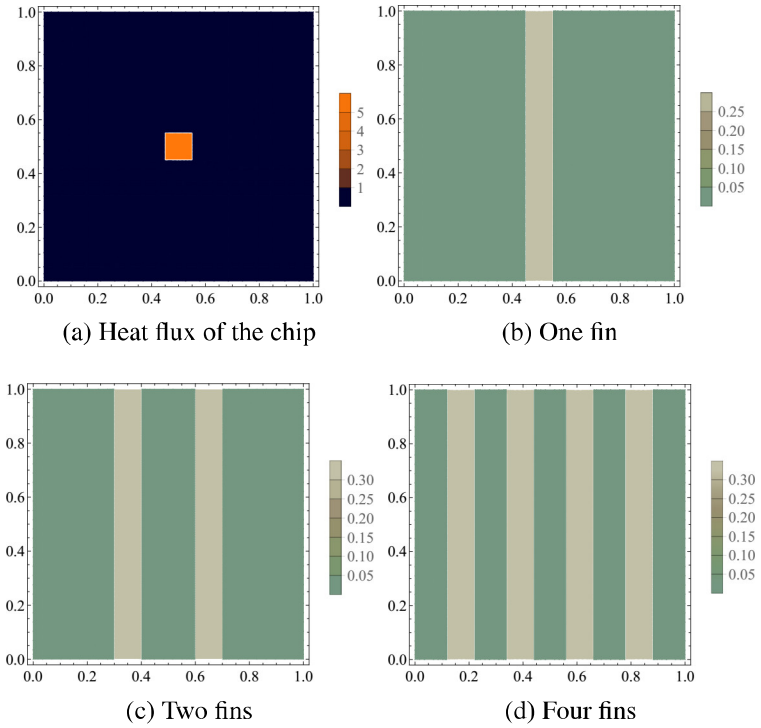

(a) Heat flux of the chip (b) One fin

(c) Two fins (d) Four fins

Figure 2: Contour plot of the heat flux and the fin layout for the considered cases

In the current work, four different layouts were tested. The first one was the heat sink without fins, under the effects of heat flux from the chip and convection only. The second has its heat dissipation increased by one fin and is shown on figure 2b. The third case introduces two fins on the heat sink. The width of the fin affects the value of Biot and, for this reason, the same width is applied in all the fins of this work. Figure 2c shows the two-fin heat sink. Finally, a four-fin layout heat sink was tested, which is a more common heat-sink layout and is shown on figure 2d. The domain of the chip and the fins are indicated on table 1.

The results of the convergence for the four different cases solved by CITT are presented in table 2. Six different positions of the heat sink were selected for the convergence analysis and because it was suspected the proximity to the chip would vary the number of the required terms to be summed for full convergence, it was selected two positions far from the chip, one in the middle of the chip, two positions very close to the boundaries of the chip and one not so far neither so close to the chip. These different positions can be seen over the domain of the base of the HS on Figure 3. The position, for instance, at the center of the heat sink and at the region where the chip is located, (0.5, 0.5), is also where the maximum temperature of the HS is found.

The first part of table 2 shows the convergence obtained for no-fins case. It can be noticed that the solution converged very fast on the far-from-chip locations. At the locations near the

Table 1: Edges of chip and fins

Components of HS	ξ_i	ξ_f	η_i	η_f
heat flux	0.45	0.55	0.45	0.55
1-fin case	0.45	0.55	0	1
2-fin case	0.3	0.4	0	1
2-fin case	0.6	0.7	0	1
4-fin case	0.12	0.22	0	1
4-fin case	0.34	0.44	0	1
4-fin case	0.56	0.66	0	1
4-fin case	0.78	0.88	0	1

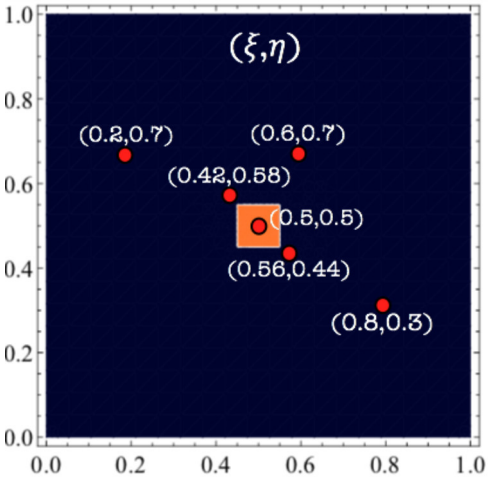

Figure 3: Different positions evaluated for the temperature convergence of the base of the HS

chip, the temperature was also higher and took more terms to converge. While 10 terms were sufficient for fully convergence at (0.2, 0.7), 200 terms were necessary for the convergence at (0.56, 0.44).

The convergence results for one-fin case is shown on the second part of the table 2. Firstly, it can be noticed a decreased on the temperature at all the selected positions of the heat sink, justifying the application of fins in order to increase the heat dissipation. As can be seen, a truncation order of $n_{\max} = 150$ was necessary for the convergence of position (0.5,0.5) while only 10 terms were necessary for the convergence for position (0.8,0.3). At (0.6,0.7), 20 terms were required for its fully convergence.

The convergence results for the two-fin heat sink layout are presented on the third part of table 2. The addiction of the second fin increased the heat dissipation and, consequently, the temperature of the heat sink was lower in this case. In this scenario, also, at the center of the heat sink, the full convergence required 250 terms instead of 150 of the previous cases. The complexity of this case may be the reason which justifies more terms to be summed. This increase of terms to be summed also happens at positions (0.42,0.58) and (0.56,0.44), which required 250 and 200 terms for these positions solution convergence.

Finally, the last part of table 2 shows the results for the four-fin layout heat sink. Similarly from the two-fin layout, more terms were necessary for the full convergence at (0.5,0.5), 350 terms in this position. In contrast, in this case, the position (0.42,0.58) had converged requiring

Table 2: Temperature $\Theta(\xi, \eta)$ convergence for different layouts of heat sink solved by CITT

No fin						
$n_{\max}$	Θ(0.2, 0.7)	Θ (0.42, 0.58)	Θ(0.5, 0.5)	Θ(0.56, 0.44)	Θ(0.6, 0.7)	Θ(0.8, 0.3)
10	0.599113	0.608526	0.619605	0.611228	0.602554	0.599113
20	0.599113	0.608530	0.619775	0.611252	0.602550	0.599113
50	0.599113	0.608526	0.619605	0.611228	0.602551	0.599113
100	0.599113	0.608526	0.619610	0.611224	0.602551	0.599113
150	0.599113	0.608526	0.619608	0.611224	0.602551	0.599113
200	0.599113	0.608526	0.619608	0.611225	0.602551	0.599113
250	0.599113	0.608526	0.619608	0.611225	0.602551	0.599113
300	0.599113	0.608526	0.619608	0.611225	0.602551	0.599113
350	0.599113	0.608526	0.619608	0.611225	0.602551	0.599113
One fin						
$n_{\max}$	Θ(0.2, 0.7)	Θ(0.42, 0.58)	Θ(0.5, 0.5)	Θ(0.56, 0.44)	Θ(0.6, 0.7)	Θ(0.8, 0.3)
10	0.153132	0.159512	0.168785	0.161935	0.153887	0.153132
20	0.153132	0.159414	0.169485	0.161726	0.153883	0.153132
50	0.153132	0.159411	0.169315	0.161702	0.153883	0.153132
100	0.153132	0.159411	0.169320	0.161698	0.153883	0.153132
150	0.153132	0.159411	0.169318	0.161698	0.153883	0.153132
200	0.153132	0.159411	0.169318	0.161699	0.153883	0.153132
250	0.153132	0.159411	0.169318	0.161699	0.153883	0.153132
300	0.153132	0.159411	0.169318	0.161699	0.153883	0.153132
Two fins						
$n_{\max}$	Θ(0.2, 0.7)	Θ(0.42, 0.58)	Θ(0.5, 0.5)	Θ(0.56, 0.44)	Θ(0.6, 0.7)	Θ(0.8, 0.3)
10	0.0763385	0.0842956	0.0948784	0.0871884	0.0782018	0.0763385
20	0.0763385	0.0841974	0.0955795	0.0869797	0.0781976	0.0763385
50	0.0763385	0.0841937	0.0954094	0.0869557	0.0781982	0.0763385
100	0.0763385	0.0841937	0.0954142	0.0869515	0.0781981	0.0763385
150	0.0763385	0.0841936	0.0954121	0.0869519	0.0781981	0.0763385
200	0.0763385	0.0841935	0.0954119	0.0869521	0.0781981	0.0763385
250	0.0763385	0.0841936	0.0954122	0.0869520	0.0781981	0.0763385
300	0.0763385	0.0841936	0.0954122	0.0869520	0.0781981	0.0763385
350	0.0763385	0.0841936	0.0954122	0.0869520	0.0781981	0.0763385
Four fins						
$n_{\max}$	Θ(0.2, 0.7)	Θ(0.42, 0.58)	Θ(0.5, 0.5)	Θ(0.56, 0.44)	Θ(0.6, 0.7)	Θ(0.8, 0.3)
10	0.0374997	0.0465666	0.057119	0.0494305	0.0405881	0.0374997
20	0.0374997	0.0464686	0.0578201	0.0492219	0.0405839	0.0374997
50	0.0374997	0.0464649	0.0576499	0.0491979	0.0405845	0.0374997
100	0.0374997	0.0464648	0.0576547	0.0491937	0.0405844	0.0374997
150	0.0374997	0.0464647	0.0576527	0.0491941	0.0405844	0.0374997
200	0.0374997	0.0464647	0.0576525	0.0491943	0.0405844	0.0374997
250	0.0374997	0.0464647	0.0576527	0.0491943	0.0405844	0.0374997
300	0.0374997	0.0464647	0.0576528	0.0491942	0.0405844	0.0374997
350	0.0374997	0.0464647	0.0576527	0.0491942	0.0405844	0.0374997
400	0.0374997	0.0464647	0.0576527	0.0491942	0.0405844	0.0374997
450	0.0374997	0.0464647	0.0576527	0.0491942	0.0405844	0.0374997

less terms, 150, and (0.6,0.7) converged summing 100 terms, the same as the previous case. The temperature along the heat sink had reduced about half from the two-fin layout, which states that the efficiency of increasing fins to heat sinks in order to increase the heat dissipation and reduce the temperature.

After analyzing the CITT convergence table 2, now it is shown the thermal profile of the solution by CITT in all the four different layouts of heat sink. The figure 4a shows the solution for the heat sink without fins, the one-fin heat sink solution is shown on figure 4b and the two-fin and four-fin layout solution are figures 4c and 4d, respectively.

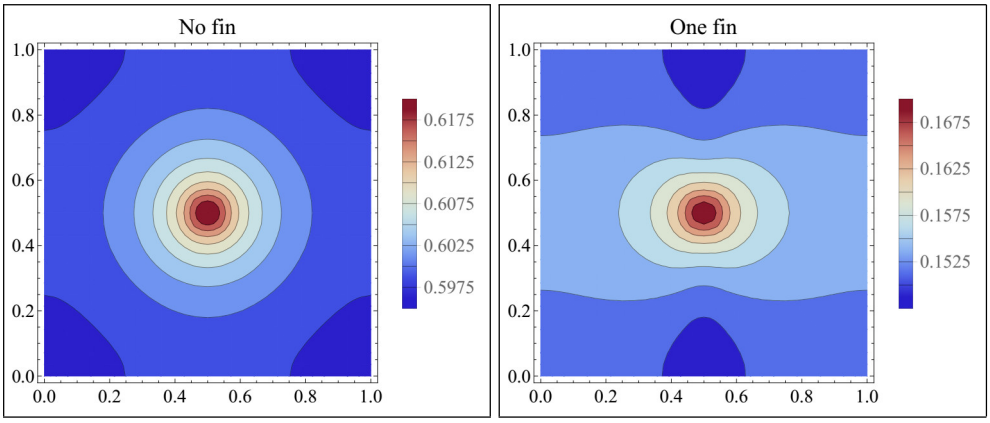

(a) Solution without any fins

(b) Solution with one fin

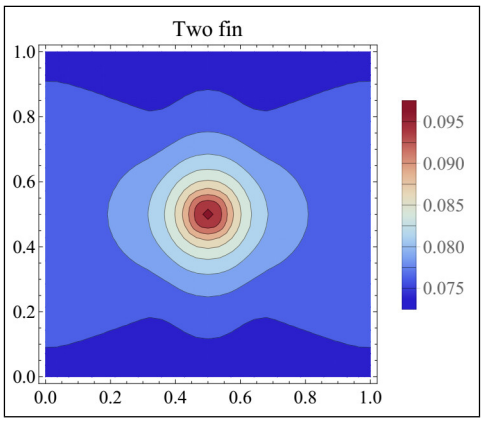

(c) Solution with two fins

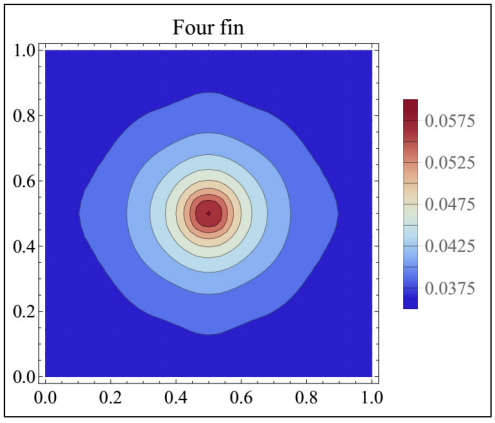

(d) Solution with four fins

Figure 4: Contour plot of the CITT solutions for the considered cases

Analyzing figure 4a, it can be noticed at first the isotherms curves around the region where the chip is located. One important detail to be noticed is also the inner dark red region, which indicates the most heated region of the base of the HS. This region indicates also the position where the chip is located, releasing heat to be dissipated. The temperature in the no-fin heat sink varies between a little more than 0.6175 and a little less than 0.5975. Figure 4b presents one fin at the center of the heat sink and the increase of the heat dissipation on the region of the fin is noticed by the darker blue stains exactly where the fin is found. The size of the inner dark red isotherm is smaller in this case, indicating again a more intense heat dissipation. Also, all the heat sink presents lower temperatures in comparison with the previous case without fins.

Figure 4c shows the solution for the two-fin case, which has a visual expressive reduction of

temperature where the fins are located, at $0.3 \leq \xi \leq 0.4$ and $0.6 \leq \xi \leq 0.7$. Also, the inner dark red region and the overall base, it presents lower temperatures from previous cases, the maximum temperature on this heat sink does not reach 0.1. Finally, the four-fin layout heat sink is shown in figure 4d. Because, this layout present equally spaced fins in all the extension of the heat sink, the thermal profile of this case resembles the no-fin case. However, the maximum temperature of the HS indicated at the inner dark red isotherm is reduced dramatically from 0.619608, of the no-fin case, to 0.0576527 with this current layout. This four-fin case is, then, the most efficient heat sink layout shown in this work, dissipating more heat and reducing the temperature for the lower values.

6 CONCLUSIONS

This paper presented the thermal analysis of a heat sink dissipating heat from a solid-state electronic solved by Classical Integral Transform Technique. The mathematical formulation of parallel plate fins was described and applied to the problem formulation for the base of the HS. The ξ dependence of the Biot number made it necessary the use of a numerical solver for the transformed problem.

The convergence analysis showed that CITT has a great performance having no difficulties to obtain high accuracy with very few terms in the solution summation far from the heat flux, and required more terms near the chip location and increasing the number of fins of the problem. The Classical Integral Transform Technique has shown to be a good alternative method for this kind of problem. Finally, the introduction of fins resulted in the expected temperature reduction. Moreover, the four-fin layout was the most efficient for dissipating heat and reducing the temperature.

Acknowledgments

The authors would like to acknowledge the financial support provided by CNPq, CAPES and FAPERJ, Brazilian agencies for the fostering of sciences.

REFERENCES

[1] A. M. Adham, N. Mohd-Ghazali and R. Ahmad. Thermal and hydrodynamic analysis of microchannel heat sinks: a review. *Renewable anf Sustainable Energies Reviews*, 21:614–622, 2013.

[2] B. C. S. Anselmo. *Análise dos Parâmetros Geométricos e Estatística Usando Minitab no Estudo da Convecção Natural em Dissipadores*. Master's Thesis, Universidade Federal de Itajubá, Itajubá – MG, Brasil, 2016.

[3] H. Azarkish, S. M. H. Sarvari and A. Behzadmehr. Optimum design of a longitudinal fin array with convection and radiation heat transfer using genetic algorithm. *International Journal of Thermal Sciences*, 49:2222–2229, 2010.

[4] N. R. Braga Junior and L. A. Sphaier. Effective thermal conductivity of composite materials using the integral transform technique. In *15th Brazilian Congress of Thermal Sciences and Engineering – ENCIT 2014*. 2014.

[5] Y. A. Çengel and A. J. Ghajar. *Heat and Mass Transfer:Fundamentals and Applications*. The McGraw-Hill Companies, Inc, 4th edition, 2011.

[6] D. J. N. M. Chalhub. *Desenvolvimento de soluções para problemas de advecção-difusão combinando transformação integral e métodos discretos*. Master's Thesis, Universidade Federal Fluminense, Niterói – RJ, Brasil, 2011.

[7] D. J. N. M. Chalhub, L. A. Sphaier and L. S. de B Alves. Integral transform analysis of poisson problems that occur in discrete solutions of the incompressible navier-stokes equations. *Journal of Physics: Conference Series*, 547:1–10, 2014.

[8] L. M. Corrêa and D. J. N. M. Chalhub. Solution of the heat conduction in solid-state electronics by integral transforms. In *24th ABCM International Congress of Mechanical Engineering - COBEM 2017*. Curitiba – PR, Brazil, 2017.

[9] P. M. Cuce and E. Cuce. Optimization of configurations to enhance heat transfer from a longitudinal fin exposed to natural convection and radiation. *International Journal of Low-Carbon Technologies*, 9:305–310, 2014.

[10] L. B. Dantas. *Heat Transfer Study of Plastic Encapsulated Chips using the Generalized Integral Transform Technique*. Master's Thesis, Universidade Federal do Rio de Janeiro, Rio de Janeiro - RJ, Brasil, 1996.

[11] F. P. Incropera. Convection heat transfer in electronic equipment cooling. *Journal of Heat Transfer, ASME*, 110:1097–1111, 1988.

[12] S. Lee, M. Early and M. Pellilo. Thermal interface material performance in microelectronic packaging applications. *Microelectronics Journal*, 28:xiii–xx, 1997.

[13] A. Lehtinen. *Analytical Treatment of Heat Sinks Cooled by Forced Convection*. D.Sc. Thesis, Tampere University of Technology, Tampere–Pirkanmaa, Finlândia, 2005.

[14] A. Malek and S. M. A. Shabani. Solving macroscopic and microscopic pin-fin heat sink problems by adapted spectral method. *Computational and Applied Mathematics*, 37(2):1112–1129, 2018.

[15] K. E. Ong, K. O. Lee, K. N. Seetharamu, I. A. Azid, G. A. Quadir, Z. A. Zainal and T. Goh. Optimization of fins used in electronic packaging. *Microelectronics International*, 22:10–15, 2005.

[16] G. P. Peterson and A. Ortega. Thermal control of electronic equipment and devices. *Advances in Heat Transfer*, 20:181–314, 1994.

[17] I. Pinheiro, L. Sphaier and L. de B. Alves. Integral transform solution of integro-differential equations in conduction-radiation problems. *Numerical Heat Transfer, Part A: Applications*, 73(2):94–114, 2018.

[18] S. Singh, D. Kumar and K. Rai. Analytical solution of fourier and non-fourier heat transfer in longitudinal fin with internal heat generation and periodic boundary condition. *International Journal of Thermal Sciences*, 125:166–175, 2018.

[19] L. Sphaier and R. Cotta. Integral transform analysis of multidimensional eigenvalue problems within irregular domains. *Numerical Heat Transfer, Part B: Fundamentals*, 38:157–179, 2000.

[20] P. Teertstra, M. M. Yovanovich and J. R. Culham. Analytical forced convection modeling of plate fin heat sinks. *Journal of Electronics Manufacturing*, 10:253–261, 2000.

[21] G. Türkakar and T. Okutucu-Özyurt. Dimensional optimization of microchannel heat sinks with multiple heat sources. *International Journal of Thermal Sciences*, 62:85–92, 2012.

[22] S. Wolfram. *The Mathematica Book*. Cambridge University Press, 2003.

[23] M. Zaretabar, H. Asadian and D. Ganji. Numerical simulation of heat sink cooling in the mainboard chip of a computer with temperature dependent thermal conductivity. *Applied Thermal Engineering*, 130:1450–1459, 2018.